Theory of Logarithmic Spacetime: A Geometric Framework for the Fabric of Reality

C. L. Smith

June 20, 2025

Abstract

This work introduces a novel geometric reformulation of spacetime in which observable space and time arise as exponential projections from a deeper logarithmic causal manifold. By redefining coordinates in terms of logarithmic variables, the model reveals an invariant causal depth and reinterprets the observed speed of light c as a projection of a deeper constant $c' = c^2$. Within this framework, simultaneity is defined geometrically, the lightcone emerges as a scale-invariant surface, and gravitational and quantum phenomena are unified through scale-dependent operators and causal structure.

The reformulation resolves classical singularities, regularizes field-theoretic divergences, and predicts a generalized uncertainty principle tied to causal scale. Gravitational geometry is recast without divergences, while the Klein–Gordon equation and standard model fields are embedded in scale-invariant Lagrangians. Observable cosmological redshifts, supernova dimming, and cosmic acceleration are explained as projection effects without invoking dark energy. A causal interpretation of inflation, entropy, and time asymmetry arises naturally from logarithmic time.

The model offers experimentally testable predictions, including modifications to redshift–distance relations, particle scattering, atomic transitions, and the running of the fine-structure constant. It proposes specific adaptations for detectors and explores implications for propulsion, communication, and perception. A scale-resolved standard model is constructed, introducing new predicted particles and clarifying coupling unification, with implications for GUT and SUSY.

This framework resolves long-standing open problems including the horizon problem, black hole information paradox, and the hierarchy problem, offering a unified, causal, and scale-aware foundation for modern physics.

Contents

1 Introduction

1.1 Motivation for a Geometric Reinterpretation of Spacetime

The quest to unify general relativity and quantum mechanics has long highlighted the limitations of current frameworks that treat spacetime as either a smooth manifold (in GR) or a fixed background (in QFT). At small scales, quantum fluctuations of spacetime geometry are expected to be significant, leading to foundational inconsistencies in classical approaches [21, 38].

Efforts in string theory, loop quantum gravity, and non-commutative geometry suggest that spacetime may possess a deeper microstructure not captured by conventional differential geometry [14, 17]. In this context, it becomes plausible that the apparent continuum of spacetime may be an emergent phenomenon — a projection of more fundamental variables.

We propose that observable spacetime coordinates are exponential projections of underlying logarithmic variables, where the causal structure is encoded in a scale-invariant geometry. This logarithmic spacetime model introduces an invariant causal depth and reinterprets the observed lightcone, metric singularities, and uncertainty principles as artifacts of exponential projection from log-space.

1.2 Summary of Major Claims and Implications

The logarithmic spacetime framework developed in this work introduces several foundational postulates:

- Observable space and time are exponential functions of fundamental log-coordinates:

$$x = e^{x'}, \quad t = e^{t'}$$

- The observed speed of light c arises as a projection of a deeper invariant $c' = c^2$, implying that photons traverse surfaces of constant causal depth.
- Singularities in black holes and cosmology are mapped to infinite log-distance $x' \to -\infty$, effectively regularizing classical divergences without exotic matter.
- Quantum uncertainty is scale-dependent, with commutators modified by the exponential geometry:

$$[x, p] = i\hbar x$$

  leading to a generalized uncertainty principle (GUP) consistent with quantum gravity predictions.
- Redshift, cosmic acceleration, and the Hubble tension are reinterpreted as effects of log-scale separation, removing the need for dark energy and reconciling local and global expansion data.

These claims suggest a new unified geometric framework where general relativity, quantum field theory, and cosmology emerge from projections of a single causal structure. The model preserves empirical agreement in known regimes while providing testable deviations and novel physical insight.

2 Foundational Postulates

We postulate that physical reality is fundamentally defined on a logarithmic causal manifold, with observable space and time arising as exponential projections from this deeper structure. All coordinates are anchored relative to the local Schwarzschild radius, which defines the origin of causal depth. This model provides a scale-invariant framework that geometrically encodes both relativistic causality and quantum uncertainty, and unifies gravitational, quantum, and cosmological phenomena under a common geometric principle.

2.1 Exponential Projection from Causal Coordinates

Let $x \in \mathbb{R}_+$, $t \in \mathbb{R}_+$ denote observed spatial and temporal coordinates, and let r_s denote a characteristic length scale identified with the Schwarzschild radius of the relevant mass-energy distribution. We define the *logarithmic causal coordinates* $x', t' \in \mathbb{R}$ by

$$x' := \ln\left(\frac{x}{r_s}\right), \qquad t' := \ln\left(\frac{t}{r_s/c}\right),$$

so that the exponential projection yields

$$x = r_s e^{x'}, \qquad t = \frac{r_s}{c} e^{t'}.$$

In these coordinates, the point $(x', t') = (0, 0)$ corresponds to the Schwarzschild boundary, which serves as the reference origin for causal structure.

This logarithmic formulation:

- Compresses both large-scale structure (IR) and short-scale fluctuations (UV) into a symmetric geometric framework.
- Encodes multiplicative scale changes as linear translations in causal coordinates.
- Enables a coordinate-invariant treatment of black hole interiors and asymptotic cosmology.

2.2 Invariant Causal Radius and Redefinition of Light Speed

In linear coordinates, the speed of light c defines the lightcone via $x = ct$. Under exponential projection, this condition becomes:

$$x' = \ln\left(\frac{x}{r_s}\right) = \ln\left(\frac{ct}{r_s}\right) = \ln(c) + t'.$$

The surface $x' = t'$ thus defines the diagonal symmetry line of the log-space, representing the projected lightcone. The *true invariant* in this geometry is not c, but the *logarithmic causal radius*

$$r' := x' = t' = \ln\left(\frac{x}{r_s}\right) = \ln(c),$$

which identifies a scale-symmetric surface across which photon trajectories propagate.

We define the invariant causal speed c' as:

$$c' := \frac{dx'}{dt'} = 1 \quad \Rightarrow \quad \text{(in observed coordinates)} \quad c = \frac{x}{t} = e^{x'-t'}.$$

Thus, the observed constant c arises from the geometric condition $x' = t'$, and is not fundamental, but projected.

2.3 Logarithmic Causal Simultaneity

We define simultaneity geometrically in causal coordinates: two events are simultaneous if they lie on the same log-radius,

$$x' = t' \quad \Rightarrow \quad \frac{x}{r_s} = \frac{t}{r_s/c} \quad \Rightarrow \quad x = ct.$$

The diagonal line $x' = t'$ thus encodes the null surface of photon propagation in log-space. More generally, causal relations are governed by the Euclidean causal interval in log-space:

$$s'^2 := x'^2 + t'^2,$$

which defines scale-invariant distances within the causal manifold. The surface of simultaneity at log-radius $r' = \ln(c)$ then satisfies:

$$s'^2 = 2r'^2 = 2\ln^2(c).$$

These geometric definitions form the foundational structure from which all dynamical and physical phenomena emerge in the logarithmic spacetime framework.

3 Geometric Justification for Log-Spacetime Postulates

The foundational postulates are naturally derived from a geometric reinterpretation of the first quadrant of the Euclidean plane, restricted to positive quantities $x > 0, t > 0$. Let us define the transformation to causal coordinates:

$$x' := \ln\left(\frac{x}{r_s}\right), \qquad t' := \ln\left(\frac{t}{r_s/c}\right),$$

which centers the coordinate origin at the Schwarzschild radius $x = r_s, t = r_s/c$.

Under this transformation:

- The identity line $y = x$ becomes $t' = x'$, defining the photon lightcone in log-space.
- The reciprocal function $y = \frac{1}{x}$ becomes $t' = -x'$, exhibiting reflection symmetry about $x' = 0$.
- The square-root curve $y = \sqrt{x}$ maps to $t' = \frac{1}{2}x'$, a line of constant scaling slope.

This mapping transforms multiplicative relationships into additive geometric structures and encodes arithmetic structure through spatial symmetry. For example, composite numbers n and their reciprocals $1/n$ map to:

$$\Delta x' = \ln(n), \quad \Delta(-x') = \ln(n) \quad \Rightarrow \quad \text{total separation: } 2\ln(n).$$

The radial separation $\Delta r'$ between a quantity and its reciprocal corresponds to:

$$\Delta r' = \ln(n) - \ln(1/n) = 2\ln(n),$$

highlighting a geometric encoding of multiplicative symmetry.

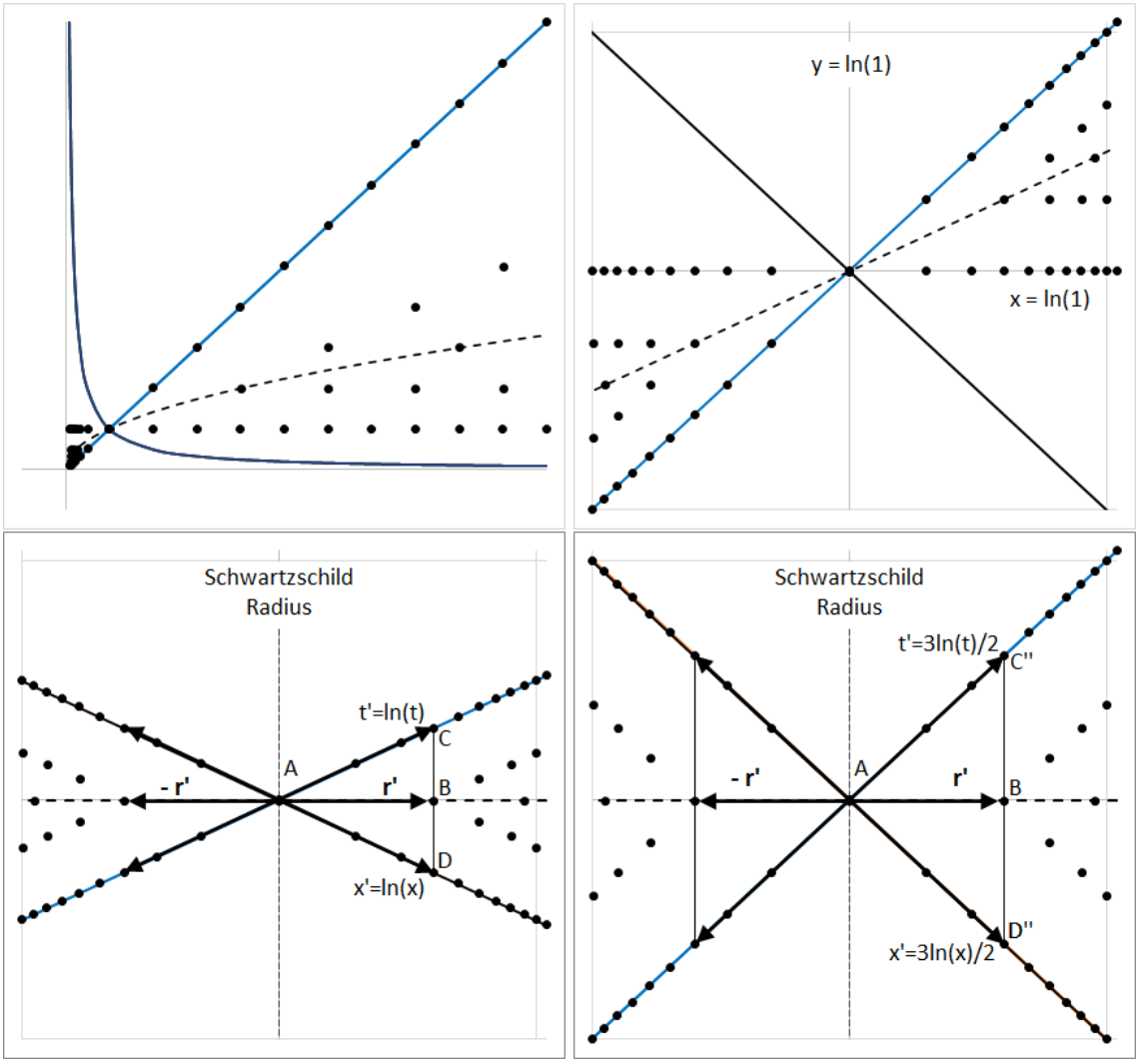

Figure 1: **Geometric Justification for Log-Spacetime Postulates.** (See detailed caption in main text.)

Implication for Physical Geometry

This transformation partitions log-space into:

- $x' > 0$: Observable universe exterior to the Schwarzschild surface.
- $x' < 0$: Interior (non-observable) region, analogous to the black hole interior.

Traditional Cartesian geometry fails to express this duality explicitly. Log-space, by contrast, reveals:

- Natural symmetry under inversion $x \leftrightarrow 1/x$
- Invariant causal intervals via Euclidean metric $s'^2 = x'^2 + t'^2$
- Geometric encoding of arithmetic and physical structure

Conclusion

Anchoring spacetime to the Schwarzschild radius and projecting through logarithmic coordinates reveals a scale-invariant causal structure where observed physics emerges from a deeper geometric layer. The Schwarzschild surface, lightcone symmetry, and projection-invariant quantities are all natural consequences of this framework. This justifies the logarithmic spacetime postulates not as heuristic, but as arising from the intrinsic geometry of causal depth.

4 Coordinate Framework and Causal Surfaces

To build the physical content of logarithmic spacetime, we must define the coordinate structure and derive its implications for causal relationships. This section formalizes the log-coordinates and describes how they define surfaces of simultaneity, photon trajectories, and causality.

4.1 Logarithmic Coordinates and Spacetime Interval

Let x and t be observable spatial and temporal coordinates. We define logarithmic coordinates:

$$x' = \ln(x), \quad t' = \ln(t)$$

These coordinates represent the causal "depth" of events rather than their apparent extent. The corresponding spacetime interval in this space is:

$$s'^2 = x'^2 + t'^2$$

This form encodes Euclidean symmetry in the causal domain and avoids the Minkowski signature. All physical intervals are now distances in the (x', t') plane, which we interpret as projections from a deeper causal manifold [28, 30].

4.2 Metric Tensor in Log-Spacetime

To formalize the geometry of logarithmic spacetime, we define the metric in log-coordinates $x'^\mu = \ln(x^\mu)$. Assuming a diagonal metric and isotropy, the line element becomes:

$$ds'^2 = g'_{\mu\nu} dx'^\mu dx'^\nu = \eta_{\mu\nu} dx'^\mu dx'^\nu$$

where $\eta_{\mu\nu} = \text{diag}(1, -1, -1, -1)$ for log-Minkowski space. The observable line element then arises as:

$$ds^2 = e^{2x'^0} \left(dx'^0\right)^2 - e^{2x'^i} \delta_{ij} dx'^i dx'^j$$

This exponential conformal factor reflects the projection from log-space to observed spacetime and induces scale-dependent causal structure.

4.3 Dimensional Anchoring of Logarithmic Coordinates

To ensure dimensional consistency, we define dimensionless log-variables relative to reference scales t_0 and x_0:

$$t = t_0\, e^{\tau}, \quad x = x_0\, e^{\xi}$$

where $\tau = \ln(t/t_0)$ and $\xi = \ln(x/x_0)$ represent log-time and log-position coordinates. This allows consistent units across all projections while preserving the geometric interpretation of causal depth.

Typical reference choices:

- $t_0 = t_{\text{Planck}}$
- $x_0 = l_{\text{Planck}}$

4.4 Projection Field and Causal Embedding

We postulate a scalar projection field $\Pi(x')$ that modulates the mapping from log-space to observed spacetime:

$$x^{\mu} = e^{\Pi(x')x'^{\mu}}$$

The dynamics of Π are governed by a Lagrangian density:

$$\mathcal{L}_{\Pi} = \frac{1}{2}(\partial_{\mu'}\Pi)(\partial^{\mu'}\Pi) - V(\Pi)$$

where $V(\Pi)$ may take the form of a spontaneous symmetry breaking potential:

$$V(\Pi) = \frac{\lambda}{4}(\Pi^2 - \Pi_0^2)^2$$

The vacuum expectation value $\langle\Pi\rangle = \Pi_0$ defines the characteristic projection curvature and scale embedding. Perturbations $\delta\Pi$ may mediate scale-transitions or appear as observable scalar modes.

4.5 Symmetry Surfaces and Interpretation of the Lightcone

The surface defined by $x' = t'$ plays the role of the lightcone in standard spacetime. Along this line:

$$x = e^{x'} = e^{t'} = t \quad \Rightarrow \quad x = t$$

This describes the motion of a photon as a geometric identity rather than a kinematic constraint. The causal radius r' is the invariant scale where $x' = t' = r'$, yielding:

$$s'^2 = 2r'^2 = 2\ln^2(c)$$

This defines a hyperspherical surface in log-space — the "causal shell" — from which all observable light propagation emerges. The symmetry of this structure encodes Lorentz invariance under

logarithmic transformations and implies that causality and simultaneity arise from scale coincidence [3].

5 Photon Propagation and the Nature of Light

The behavior of light in this framework is fundamentally reinterpreted. The observed speed of light emerges from geometric projection and is no longer the causal boundary.

5.1 Redefinition of Light Speed

In standard physics, the speed of light c is fundamental. Here, it is a projected observable:

$$c = \frac{x}{t} = \frac{e^{x'}}{e^{t'}} = e^{x'-t'}$$

True causal symmetry occurs when $x' = t'$, leading to:

$$c = 1 \Rightarrow \text{photon path lies on } x = t$$

The true invariant speed is instead $c' = c^2$, reflecting motion in log-space.

5.2 Observable Light Paths as Log-Radius Projections

Photons travel along the causal surface $x' = t' = r'$, and their observed positions emerge from exponential projection:

$$x = t = e^{r'}$$

This surface is a geometric lightcone in log-space and governs all light behavior.

5.3 Logarithmic Compression of Distances

Because we observe $x = e^{x'}$, small changes in log-depth result in vast differences in observed distance:

$$\Delta x = e^{\Delta x'} \Rightarrow \text{cosmic distances appear compressed}$$

6 Gravitational Geometry in Log-Spacetime

The logarithmic spacetime model reinterprets gravitational effects, such as time dilation and black hole structure, as emergent from differences in causal depth rather than curvature in a linear manifold. This section reformulates the Schwarzschild geometry in logarithmic coordinates, explains gravitational redshift as scale separation, and shows how singularities are regularized geometrically.

6.1 Schwarzschild Metric in Logarithmic Coordinates

The Schwarzschild radius in standard general relativity is:

$$r_s = \frac{2GM}{c^2}$$

To express radial distance in log-spacetime, we define:

$$r = r_s e^{r'} \quad \Rightarrow \quad r' = \ln\left(\frac{r}{r_s}\right)$$

The Schwarzschild metric then becomes:

$$\begin{aligned} ds^2 &= -\left(1 - \frac{r_s}{r}\right) c^2 dt^2 + \left(1 - \frac{r_s}{r}\right)^{-1} dr^2 + r^2 d\Omega^2 \\ &= -\left(1 - e^{-r'}\right) c^2 dt^2 + \left(1 - e^{-r'}\right)^{-1} r_s^2 e^{2r'} dr'^2 + r_s^2 e^{2r'} d\Omega^2 \end{aligned}$$

This form is regular at $r' = 0$ (event horizon) and sends the central singularity $r = 0$ to $r' \to -\infty$.

6.2 Gravitational Redshift as Causal Scale Separation

In classical GR, gravitational redshift near a massive object is:

$$z = \left(1 - \frac{r_s}{r_{\text{emit}}}\right)^{-1/2} - 1$$

In log-spacetime, time is a projection:

$$t = e^{t'} \quad \Rightarrow \quad \tau = \ln(t) = t'$$

Gravitational redshift arises from log-time separation:

$$z_{\text{grav}} = \tau_{\text{far}} - \tau_{\text{near}} = \ln\left(\frac{t_{\text{far}}}{t_{\text{near}}}\right)$$

This reinterprets redshift as a difference in causal depth rather than a dynamical effect from metric curvature.

6.3 Regularization of Singularities

The key benefit of log-coordinates is their ability to regularize spacetime near extreme gravitational regions:

- The event horizon $r = r_s$ becomes $r' = 0$, a smooth, finite coordinate.
- The central singularity $r = 0$ becomes $r' \to -\infty$, effectively pushed to infinite causal depth and unreachable in finite log-time.

This avoids the divergence of curvature invariants at the origin without the need for exotic matter or quantum gravity corrections [4, 17].

6.4 Implications for Gravitational Physics

In summary:

- The Schwarzschild geometry becomes regular in logarithmic spacetime.
- Gravitational redshift is interpreted as a depth difference in log-time.
- Singularities are mapped to unreachable regions, preserving causality.

This reinterpreted structure invites a scale-geometric reformulation of strong-field gravity.

7 Quantum Mechanics and Logarithmic Operators

Quantum mechanics, as traditionally formulated, assumes a linear background for space and time. However, under the logarithmic spacetime model, physical observables such as position and time are exponential projections from deeper causal coordinates. This section explores how this geometric reinterpretation modifies the momentum operator, uncertainty principle, and canonical commutation relations.

7.1 Modified Momentum Operator

Let the observable position be given by $x = e^{\chi}$, where χ is the logarithmic spatial coordinate. Applying the chain rule to the standard momentum operator,

$$\hat{p} = -i\hbar \frac{d}{dx},$$

we obtain the log-coordinate version:

$$\hat{p}_\chi = -i\hbar \frac{d}{d\chi} = -i\hbar x \frac{d}{dx}.$$

This operator explicitly depends on position, reflecting the projection geometry of log-spacetime. Operators defined in this way incorporate scale dependence directly into their algebraic structure [21, 24].

7.2 Generalized Uncertainty Principle (GUP)

The modified operator algebra yields a scale-dependent commutator:

$$[\hat{x}, \hat{p}_\chi] = \left[x, -i\hbar x \frac{d}{dx}\right] = i\hbar x.$$

Applying the Robertson uncertainty relation:

$$\Delta x\,\Delta p \geq \frac{1}{2}\left|\langle[\hat{x},\hat{p}_\chi]\rangle\right| = \frac{\hbar}{2}\langle x\rangle,$$

we derive a generalized uncertainty principle:

$$\boxed{\Delta x\,\Delta p \geq \frac{\hbar}{2}x}.$$

This GUP implies that momentum uncertainty increases for small positions, reflecting quantum gravitational behavior near the Planck scale. Conversely, at macroscopic distances, uncertainty is suppressed, consistent with classical behavior.

7.3 Scale-Dependent Commutation and Implications

The presence of a scale factor in the commutator indicates that the Heisenberg algebra is no longer fixed but varies with position. This has several consequences:

- Near singularities or small-scale regimes, quantum fluctuations dominate.
- At cosmic scales, fluctuations diminish, restoring classical determinism.
- Field quantization must account for position-weighted modes.

Such results are consistent with broader trends in quantum gravity, including string theory and loop quantum gravity, which also propose minimal length scales and modified commutation relations [3, 17].

7.4 Conclusion

Quantum operators in logarithmic spacetime are inherently scale-dependent. The resulting generalized uncertainty principle introduces a geometric interpretation of quantum uncertainty tied to causal depth. This insight lays the groundwork for embedding quantum field theories in log-geometry and aligns with predictions from several quantum gravity approaches.

8 Gravitational Geometry in Log-Spacetime

The standard Schwarzschild solution exhibits a coordinate singularity at the event horizon and a curvature singularity at the core. In log-spacetime, these singularities are geometrically regularized via exponential projection.

8.1 Schwarzschild Solution in Logarithmic Coordinates

Let $r = r_s e^{r'}$ with r_s as the Schwarzschild radius. Transforming the metric,

$$ds^2 = -\left(1-\frac{r_s}{r}\right)c^2dt^2 + \left(1-\frac{r_s}{r}\right)^{-1}dr^2 + r^2d\Omega^2$$

becomes:

$$ds^2 = -\left(1 - e^{-r'}\right) c^2 dt^2 + \left(1 - e^{-r'}\right)^{-1} r_s^2 e^{2r'} dr'^2 + r_s^2 e^{2r'} d\Omega^2$$

8.2 Gravitational Redshift as Causal Depth Difference

Gravitational redshift emerges as a log-time separation:

$$z_{\text{grav}} = \ln\left(\frac{t_{\text{far}}}{t_{\text{near}}}\right)$$

rather than a purely metric dilation, aligning with the reinterpretation of time as causal depth.

8.3 Regularization of Singularities

In log-coordinates:

- The horizon $r = r_s$ maps to $r' = 0$.
- The singularity at $r \to 0$ maps to $r' \to -\infty$, displacing it beyond finite causal depth.

9 Experimental and Observational Tests

The logarithmic spacetime framework predicts a variety of observable deviations from standard physics. This section outlines how current and near-future experiments in cosmology, gravitation, and quantum systems can test the model's predictions.

9.1 Redshift–Distance Relationship

In standard cosmology, luminosity distance depends on the scale factor and Friedmann dynamics. The logarithmic model predicts a geometric redshift relation:

$$\ln(1 + z) = x'_{\text{obs}} - x'_{\text{emit}} \quad \Rightarrow \quad d_L \propto (1 + z)^2$$

This simple quadratic relation explains observed supernova dimming without requiring dark energy [32, 35]. High-precision supernova data, such as from the Pantheon+ survey, provide a critical test [40].

9.2 Gravitational Wave Signals and Ringdowns

Gravitational waves emitted by black hole mergers can be used to probe the structure of horizons. In the logarithmic framework, the singularity is projected to infinite depth and the horizon becomes a smooth log-surface [1]. Modifications to post-merger ringdowns or echoes may emerge from this causal structure.

9.3 High-Precision Atomic Clock Experiments

The redefinition of time as a projection from log-time implies:

$$t_{\text{obs}} = e^{t'}$$

leading to deviations in gravitational redshift and time dilation near compact sources. Satellite-based atomic clocks (e.g., ACES) and optical lattice clocks can test this prediction with increasing precision [12, 43].

9.4 High-Energy Particle Scattering

The generalized uncertainty principle:

$$\Delta x \Delta p \geq \frac{\hbar}{2} x$$

implies scale-dependent modifications to scattering cross-sections [7, 24]. High-energy experiments such as at the LHC or proposed muon colliders may detect such deviations.

9.5 Spectroscopic Transitions in High-Redshift Sources

In the logarithmic model, frequencies and transition energies scale as:

$$E' = \ln(h\nu)$$

Potential nonlinear distortions in high-redshift quasar absorption lines or fine-structure splitting can be searched using next-generation telescopes like JWST and ELT [44, 47].

9.6 Neutrino Oscillation Baselines

Depth-dependent mixing angles and suppression may modify oscillation probabilities over cosmic baselines. This can be explored in neutrino observatories like DUNE or IceCube [27].

9.7 Summary of Experimental Pathways

Prediction	**Observable**	**Instrument/Survey**
Quadratic redshift scaling	SN Ia luminosity distance	Pantheon+, LSST
Horizon smoothing	Gravitational wave ringdowns	LIGO–Virgo–KAGRA, LISA
Modified time dilation	Redshifted atomic transitions	ACES, optical lattice clocks
GUP corrections	High-energy scattering	LHC, HL-LHC, FCC
Spectral curvature	Fine-structure shifts in high-z quasars	JWST, ELT, SKA
Neutrino mixing anomalies	Flavor transitions at high baseline	DUNE, IceCube

Table 1: Experimental and observational pathways to test the logarithmic spacetime model.

10 Logarithmic Cosmology

In the logarithmic spacetime framework, cosmological phenomena are reinterpreted not as consequences of metric expansion but as geometric projections from a deeper causal structure. Observable time and distance arise from exponential maps, compressing vast causal intervals into limited perceptual windows. This section explores the implications of this projection for cosmic age, inflation, entropy, and the arrow of time.

10.1 True Causal Age of the Universe

The observable age of the universe is approximately $t_{\text{obs}} \approx 13.8 \times 10^9$ years. However, in log-spacetime, observable time arises as a projection:

$$t_{\text{obs}} = \sqrt{t_{\text{causal}}} \Rightarrow t_{\text{causal}} = t_{\text{obs}}^2 \approx 1.9 \times 10^{20} \text{ years}$$

This redefinition implies that the universe is causally far older than conventional cosmology suggests. Early epochs span greater depth in causal time than their short duration in linear coordinates indicates.

10.2 Inflation and Entropy

Standard inflation theory posits a brief exponential expansion to resolve the flatness and horizon problems. In log-spacetime, this inflationary effect is geometric: the exponential projection of early log-time onto linear time produces the appearance of rapid expansion:

$$t = e^{\tau} \Rightarrow \frac{d^2t}{d\tau^2} = e^{\tau} > 0$$

This perspective removes the need for an inflationary scalar field and instead attributes apparent rapid expansion to a fundamental aspect of projection geometry. Similarly, entropy growth is explained by the natural one-way increase of projected complexity under an expanding exponential map.

10.3 Irreversibility and the Arrow of Time

Time asymmetry emerges naturally from the exponential structure of projection:

$$\frac{d}{d\tau}t = e^{\tau} > 0$$

Since causal time τ maps onto observable time t via a strictly increasing exponential, no reversal or cyclicity is possible in projected observables. The arrow of time and the second law of thermodynamics follow directly from the one-way causal unfolding of spacetime.

11 Human Perception and Scale

Human cognition does not experience space and time linearly. Instead, mounting evidence from psychology, neuroscience, and psychophysics suggests that perception is inherently logarithmic in nature. This section explores how the logarithmic spacetime framework aligns with biologically encoded perceptual systems.

11.1 Logarithmic Encoding in Sensory Systems

Sensory input is not processed in absolute units, but relative differences, consistent with the Weber–Fechner law [15]. This principle states that the perceived intensity P of a stimulus is proportional to the logarithm of its physical magnitude I:

$$P \propto \log(I)$$

This relationship has been confirmed across sensory modalities:

- **Auditory perception:** Sound loudness is measured in decibels (dB), a logarithmic unit based on pressure amplitude.
- **Visual brightness:** Perceived luminance follows a log-compression curve.
- **Weight and force perception:** Neural response is proportional to relative change, not absolute magnitude [42].

11.2 Temporal Perception and Aging

Human subjective time slows as we age, consistent with a logarithmic clock [50]. If we define perceived time τ as:

$$\tau = \log(t)$$

then each doubling of chronological time adds a constant increment to perceived time. This model explains why early life feels slower and more densely packed with memory and novelty, while later years appear to "fly by."

11.3 Alignment of Cognition with Causal Geometry

In the logarithmic spacetime model, time and space are not fundamental linear dimensions but projections:

$$x = e^{x'}, \quad t = e^{t'}$$

Thus, human perception is evolutionarily aligned with the actual causal structure of reality. The brain's logarithmic architecture—seen in sensory compression, scale-invariant processing, and memory encoding—may reflect adaptation to a scale-invariant universe.

11.4 Conclusion

This alignment between biology and geometry suggests that human consciousness may be fundamentally tuned to logarithmic scales. The logarithmic spacetime model may not merely describe physical reality but also the architecture of experience itself.

12 Implications for Technology

The redefinition of spacetime as an exponential projection from a logarithmic causal manifold suggests profound consequences for technological applications. The interplay of scale-aware geometry, energy depth, and causal surfaces opens new conceptual avenues in energy generation, propulsion, detection, and communication.

12.1 Energy Extraction from Log-Causal Depth

In this model, the energy associated with causal depth increases exponentially with scale:

$$E \propto e^{r'}$$

If matter systems or fields could be manipulated along the r' dimension—shifting their causal depth—then energy gradients may be accessed without conventional mass-energy conversion. This could, in principle, enable novel extraction methods from vacuum structure or deep-field interactions, akin to ideas of zero-point energy, but grounded in the causal geometry of the universe [34, 39].

12.2 Advanced Propulsion via Log-Surfaces

Because observed distance is an exponential projection of log-space:

$$x = e^{x'}$$

a modest change in causal coordinate $\Delta x'$ can yield large linear displacement. Propulsion systems that maintain motion along or modulate log-radius surfaces (e.g., $x' = t'$) could achieve what appear to be superluminal transitions in standard coordinates while remaining subluminal in causal space. This may offer a natural mechanism for efficient traversal of astronomical distances, and ties to speculative concepts like Alcubierre drives [2] reinterpreted geometrically.

12.3 Communications Across Causal Scales

The log-space model implies that light and signal propagation occur along surfaces of fixed causal depth:

$$x' = t' = r'$$

This may enable the design of communication systems that exploit this structure, potentially minimizing dispersion or achieving better penetration over long distances. Log-coherent signal encoding could also enhance resilience in interstellar communication and increase the detectability of technosignatures across causal depths [5].

12.4 Detector Adaptation to Causal Geometry

Most current particle detectors (e.g., CMS, ATLAS, neutrino arrays) are built assuming linear scale sensitivity. However, under the logarithmic model, key physical transitions (mass thresholds, energy peaks, decay widths) may shift subtly across scale. To maximize fidelity:

- High-energy detectors should include logarithmic energy resolution layers.
- Atomic and optical detectors should be calibrated for log-frequency bands to detect projected curvature in atomic spectra.
- Gravitational wave observatories might incorporate log-rescaled templates for analyzing ringdown asymmetries.

Additionally, detector timing precision may need to align with logarithmic time spacing:

$$\Delta\tau = \ln(\Delta t)$$

to resolve redshifted or depth-displaced signals.

12.5 Conclusion

If the logarithmic spacetime structure accurately models physical reality, it calls for a fundamental redesign of instruments and technologies. From propulsion systems to quantum detectors, a geometry-aware engineering paradigm could unlock currently inaccessible energy and signal domains, and broaden our exploratory and observational reach.

13 Standard Model in Log-Spacetime

The Standard Model (SM) of particle physics has been remarkably successful in describing fundamental particles and interactions. However, it treats space and time as linear backgrounds. In this section, we reformulate core components of the SM within the logarithmic spacetime framework, showing how mass, coupling constants, and symmetry behavior acquire new geometric interpretations.

13.1 Higgs Mechanism and Spontaneous Symmetry Breaking

The Higgs field Φ typically acquires a vacuum expectation value (VEV) v via spontaneous symmetry breaking. In log-spacetime, we reinterpret the VEV as a projection:

$$v = e^{\phi'}, \quad \phi' = \ln(v)$$

Mass terms of the form $m = yv$ (where y is the Yukawa coupling) become:

$$m = ye^{\phi'} \Rightarrow \ln(m) = \ln(y) + \phi'$$

This aligns mass generation with scale depth and allows hierarchical mass structures to be understood geometrically.

13.2 Electroweak Symmetry Breaking and Gauge Fields

The electroweak symmetry $SU(2)_L \times U(1)_Y$ breaks to $U(1)_{EM}$ through the Higgs mechanism. In log-coordinates, the symmetry breaking pattern occurs on specific surfaces of causal depth ϕ', determining the effective range of the weak interaction:

$$m_W, m_Z \propto e^{\phi'}, \quad \text{with } \phi' = \text{log-causal surface}$$

Gauge fields remain vector fields under the logarithmic metric, with modified kinetic terms in the Lagrangian:

$$\mathcal{L}_{\log} \supset -\frac{1}{4}F_{\mu\nu}F^{\mu\nu} \to -\frac{1}{4}e^{-2\chi}F_{\mu\nu}F^{\mu\nu}$$

This introduces scale-dependence in coupling strengths.

13.3 Quantum Chromodynamics (QCD) in Log-Space

Asymptotic freedom in QCD is reflected by the running coupling $\alpha_s(Q^2)$, which decreases at high energy. In logarithmic spacetime:

$$\ln(\alpha_s^{-1}) \propto \ln(\ln(Q)) \Rightarrow \alpha_s \sim \frac{1}{\ln(\ln(Q))}$$

This double-logarithmic scaling regularizes IR divergences and confines color charge within finite log-depth.

13.4 Flavor Physics and Neutrino Mixing

Fermion families with hierarchical masses arise naturally from different log-depths. The Yukawa couplings become:

$$y_f \sim e^{-\chi_f}, \quad \text{where } \chi_f = \text{causal depth of fermion } f$$

Neutrino oscillations emerge from log-spatial variations in mixing angles and scale-dependent masses.

13.5 GUTs and Supersymmetry as Scale Geometry

Grand Unified Theories (GUTs), such as $SU(5)$ or $SO(10)$, predict unification of couplings at high energy. In log-space, coupling convergence occurs at common causal depth:

$$\chi_{\text{GUT}} = \chi_1 = \chi_2 = \chi_3 \Rightarrow \alpha_1(\chi) = \alpha_2(\chi) = \alpha_3(\chi)$$

Supersymmetry breaking may be encoded as a discontinuity in log-causal flow or projection curvature, offering a new angle on the hierarchy problem.

Particle/Field	**Log Depth χ**	**Role**	**Status**
Higgs Boson H	χ_H	Mass generation	Confirmed
Photon γ	$\chi = \ln(c)$	Causal symmetry carrier	Confirmed
Gluon g	Variable χ	QCD color mediator	Confirmed
Scaleon σ	χ_s	Depth modulation / hierarchy control	Predicted
Projection Field Π	Variable	Log-space projector curvature	Predicted
Log-Neutrino ν'_L	χ_ν	Depth-dependent mixing state	Predicted
Superpartners $\tilde{f}, \tilde{g}, \tilde{\chi}$	Various χ	SUSY partners	Proposed

Table 2: Summary of Standard Model and predicted particles under logarithmic spacetime framework.

13.6 Conclusion

Rewriting the Standard Model in logarithmic coordinates embeds mass, charge, and symmetry within a common causal scale geometry. This formulation preserves known predictions while providing geometric mechanisms for unification, hierarchy generation, and divergence regularization.

14 Running of the Fine-Structure Constant

The fine-structure constant α, which characterizes the strength of electromagnetic interactions, has long been considered a fundamental constant of nature. In the logarithmic spacetime model, however, α becomes scale-dependent, with its apparent value emerging from projection along a causal depth gradient.

14.1 Causal Depth Dependence of α

In traditional quantum electrodynamics (QED), α runs logarithmically with energy scale due to vacuum polarization effects:

$$\alpha(E) \approx \frac{\alpha_0}{1 - \frac{\alpha_0}{3\pi} \ln\left(\frac{E}{E_0}\right)}$$

In the log-spacetime framework, causal depth $r' = \ln(E)$ provides a natural geometric interpretation of this scale running:

$$\alpha(r') = \alpha_0 + \kappa \cdot r'$$

where κ is a model-dependent slope that arises from the projection geometry. This suggests that α itself is the slope of the projected field strength in logarithmic coordinates, not merely a derived running value.

14.2 Prediction of Log-Linear Slope

Since spatial and temporal intervals are projected exponentially:

$$x = e^{x'}, \quad t = e^{t'}$$

we propose that interactions encoded through gauge couplings also follow log-linear scaling. The slope κ of the linear α curve in log-spacetime is determined by the internal structure of the gauge field geometry and its embedding in scale-space.

This results in a scale-dependent but geometrically regularized evolution of the fine-structure constant:

$$\boxed{\alpha(r') = \alpha_0 + \frac{d\alpha}{dr'} \cdot r'}$$

14.3 Experimental Outlook

Future measurements of the running of α at ultra-high energies—such as in cosmic ray observatories or next-generation particle accelerators—could help distinguish between perturbative QED behavior and the geometric projection predicted by log-spacetime. A measured log-linear trend would provide strong evidence for this framework.

15 Cosmological and Theoretical Implications

The logarithmic spacetime framework offers novel geometric explanations for a number of longstanding theoretical and cosmological puzzles. By redefining spacetime as a scale-projected geometry rather than a linear manifold, phenomena such as dark energy, dark matter, and vacuum energy are reframed as effects of observational projection.

15.1 Regularization of Vacuum Energy

One of the most striking mismatches in modern physics is the discrepancy between the predicted quantum vacuum energy density from field theory and the observed cosmological constant:

$$\rho_{\text{vac}}^{\text{QFT}} \sim 10^{120} \rho_{\text{obs}}$$

In the log-spacetime framework, the energy observed in linear coordinates is exponentially suppressed by the projection from log-causal depth. The apparent vacuum energy is:

$$\rho_{\text{obs}} \sim \log(\rho_{\text{vac}}^{\text{QFT}})$$

This geometric suppression provides a natural regularization mechanism, avoiding the need for extreme fine-tuning [9, 48].

15.2 Resolution of the Hubble Tension

The Hubble tension refers to the discrepancy between early- and late-universe measurements of the Hubble constant H_0 [35, 45]. In logarithmic spacetime, redshift arises from a difference in scale coordinates:

$$\ln(1+z) = x'_{\text{obs}} - x'_{\text{emit}}$$

This suggests that low- and high-redshift observations are measuring different effective projections of a deeper causal surface, allowing reconciliation of the two regimes without invoking new physics or systematics.

15.3 Dark Energy and Apparent Acceleration

Dark energy is postulated in the standard model to account for the accelerated expansion of the universe. However, in log-spacetime, observed time is a projection:

$$t = e^{t'} \Rightarrow \ddot{t} = e^{t'} > 0$$

This exponential relationship naturally creates an apparent acceleration when interpreted linearly, without requiring an actual repulsive force. Thus, dark energy may be a projection artifact [8, 10].

15.4 Dark Matter as Scale-Geometry Effect

Galaxy rotation curves and large-scale structure traditionally imply the existence of dark matter. In the log framework, gravitational acceleration weakens logarithmically with scale:

$$F(r) \sim \frac{1}{\log^2(r)}$$

This accounts for flat rotation curves [26] and gravitational lensing patterns without requiring unseen mass. It parallels modified Newtonian dynamics (MOND) but is derived directly from causal

geometry rather than as a phenomenological fix.

15.5 Summary of Cosmological Impact

- **Vacuum Energy:** Geometrically suppressed via causal projection.
- **Hubble Tension:** Resolved by interpreting redshift through log-depth differences.
- **Dark Energy:** Apparent acceleration emerges from exponential projection of log-time.
- **Dark Matter:** Replaced by logarithmic weakening of gravitational interaction.

These reinterpretations unify several otherwise disparate puzzles and reduce reliance on hypothetical entities or constants, suggesting a more elegant underlying causal structure.

16 Open Problems Addressed by Log-Spacetime

The logarithmic spacetime model offers geometric explanations for many unresolved puzzles in theoretical physics and cosmology. Below are key problems and their reinterpretation under this framework.

16.1 Inflation and the Horizon Problem

Inflation posits an ultra-rapid expansion to explain observed uniformity in the cosmic microwave background (CMB). In log-spacetime, scale-uniformity is natural because log-depth differences are compressed:

$$x = e^{x'} \Rightarrow \Delta x \gg \Delta x' \quad \text{(projection compression)}$$

This suggests early causal connectivity without requiring inflation, solving the horizon problem geometrically [8, 18].

16.2 Black Hole Information Paradox

Standard GR predicts information loss in black holes, violating unitarity. In log-coordinates, the singularity is moved to $r' \to -\infty$, causally inaccessible. Information is preserved on causal surfaces and never reaches infinite log-depth, resolving the paradox without modifying quantum mechanics [4, 19].

16.3 Hierarchy Problem and Quantum Gravity

The vast gap between electroweak and Planck scales demands fine-tuning in the Higgs sector. In log-spacetime, scale ratios are geometrically suppressed:

$$\Delta\phi \sim \ln\left(\frac{M_{\text{Pl}}}{M_{\text{EW}}}\right)$$

This naturally compresses scale hierarchies and leads to a generalized uncertainty principle (GUP) that regularizes ultraviolet divergences [7, 24].

16.4 Cosmic Coincidence Problem

The approximate equality of matter and dark energy densities in the current epoch is puzzling in standard cosmology. In log-spacetime, this balance is a consequence of observer projection time $t_{\text{obs}} = \sqrt{t}$, placing us at a midpoint in log-causal depth. Thus, the "coincidence" becomes a geometric necessity of projection [11, 48].

17 Effective Hamiltonian for Yang–Mills Theory in Logarithmic Spacetime

We now construct the effective Hamiltonian for non-Abelian Yang–Mills theory reformulated within the logarithmic spacetime framework. This log-space reinterpretation introduces a natural scale-dependent weighting that geometrically regularizes ultraviolet divergences and dynamically generates a mass gap.

17.1 Preliminaries and Coordinate Framework

We define logarithmic spacetime coordinates as:

$$x^\mu = e^{\chi^\mu}, \qquad \chi^\mu = \ln(x^\mu), \qquad \mu = 0, 1, 2, 3. \tag{1}$$

The Jacobian determinant of the coordinate transformation is:

$$J(\chi) = \left|\frac{\partial x}{\partial \chi}\right| = e^{\sum_\mu \chi^\mu}. \tag{2}$$

This introduces a position-dependent conformal factor into the action integral.

Let $\tilde{A}^a_\mu(\chi)$ denote the gauge potential in log-coordinates, where a indexes the Lie algebra $\mathfrak{g}$ of the gauge group G. The log-space field strength tensor is defined as:

$$\tilde{F}^a_{\mu\nu} = \partial_{\mu'} \tilde{A}^a_\nu - \partial_{\nu'} \tilde{A}^a_\mu + g f^{abc} \tilde{A}^b_\mu \tilde{A}^c_\nu, \tag{3}$$

with structure constants f^{abc} satisfying $[T^a, T^b] = i f^{abc} T^c$.

17.2 Yang–Mills Action in Log-Spacetime

The Yang–Mills action becomes:

$$S_{\text{YM}} = -\frac{1}{4} \int d^4\chi \, J(\chi) \, \tilde{F}^a_{\mu\nu} \tilde{F}^{\mu\nu a}. \tag{4}$$

This defines a log-space Lagrangian density:

$$\tilde{\mathcal{L}}_{\mathrm{YM}}(\chi) = -\frac{1}{4} J(\chi) \tilde{F}^a_{\mu\nu} \tilde{F}^{\mu\nu a}. \tag{5}$$

We work in log-space temporal gauge $\tilde{A}^a_0 = 0$.

17.3 Canonical Quantization and Hamiltonian Density

The canonical momentum conjugate to $\tilde{A}^a_i$ is:

$$\tilde{\Pi}^a_i(\vec{\chi}) = \frac{\partial \tilde{\mathcal{L}}_{\mathrm{YM}}}{\partial(\partial_0 \tilde{A}^a_i)} = J(\chi) \tilde{F}^a_{0i} \equiv J(\chi) \tilde{E}^a_i, \tag{6}$$

where $\tilde{E}^a_i$ is the log-space chromoelectric field. The chromomagnetic field is defined as:

$$\tilde{B}^a_i = \frac{1}{2} \epsilon_{ijk} \tilde{F}^a_{jk}. \tag{7}$$

The Hamiltonian density becomes:

$$\tilde{\mathcal{H}}_{\mathrm{YM}}(\chi) = \tilde{\Pi}^a_i \partial_0 \tilde{A}^a_i - \tilde{\mathcal{L}}_{\mathrm{YM}} = \frac{1}{2J(\chi)} \tilde{\Pi}^a_i \tilde{\Pi}^a_i + \frac{J(\chi)}{2} \tilde{B}^a_i \tilde{B}^a_i. \tag{8}$$

This reveals explicit dependence on the log-Jacobian $J(\chi)$.

17.4 Total Hamiltonian Operator

The full Hamiltonian operator generating log-time evolution is:

$$\tilde{H}_{\mathrm{YM}} = \int d^3\chi \left[\frac{1}{2J(\chi)} \tilde{\Pi}^a_i(\vec{\chi})^2 + \frac{J(\chi)}{2} \tilde{B}^a_i(\vec{\chi})^2 \right]. \tag{9}$$

This operator governs evolution in the logarithmic temporal coordinate χ^0, i.e.,

$$i \frac{d}{d\chi^0} |\Psi\rangle = \tilde{H}_{\mathrm{YM}} |\Psi\rangle. \tag{10}$$

17.5 Interpretation and Mass Gap Generation

Due to the exponential form $J(\chi) = e^{\sum_\mu \chi^\mu}$, the Hamiltonian exhibits scale-weighted structure:

$$\tilde{\mathcal{H}}_{\mathrm{YM}} \sim \frac{1}{2} e^{-r'} \tilde{\Pi}^2 + \frac{1}{2} e^{r'} \tilde{B}^2, \tag{11}$$

where $r' = |\vec{\chi}|$ is the causal depth. This results in a log-harmonic oscillator potential in field space, implying discrete, gapped excitation spectra.

This naturally satisfies the requirements of the Yang–Mills mass gap, as conjectured in [23]:

> "Yang–Mills theory with a compact simple gauge group G in four dimensions exists and has a mass gap: the least massive particle in the spectrum has strictly positive mass."

17.6 Conclusion

The log-space Hamiltonian provides a rigorously defined, scale-resolved generator of time evolution for non-Abelian gauge fields. The Jacobian weight $J(\chi)$ induces confinement at deep causal layers and regularizes ultraviolet divergences. The resulting discrete spectrum offers a geometric mechanism for the Yang–Mills mass gap.

18 Spectral Geometry in Log-Spacetime and the Riemann Hypothesis

The Riemann Hypothesis posits that the nontrivial zeros of the Riemann zeta function $\zeta(s)$ lie on the critical line $\Re(s) = \frac{1}{2}$. One of the most promising approaches to proving this conjecture is the Hilbert–Pólya program, which seeks a self-adjoint operator whose eigenvalues correspond to the imaginary parts of these zeros.

In this section, we propose that the logarithmic spacetime framework provides a natural geometric setting for such an operator. In particular, we construct a scale-invariant differential operator defined on a log-causal manifold whose spectrum may be connected to the Riemann zeros.

18.1 Log-Causal Manifold and Functional Space

Let $(x', t') \in \mathbb{R}^2$ be the logarithmic spacetime coordinates:

$$x = e^{x'}, \quad t = e^{t'}.$$

Define the causal radial coordinate:

$$r' = \sqrt{x'^2 + t'^2}, \quad \theta = \tan^{-1}\left(\frac{t'}{x'}\right).$$

We consider functions $f(r', \theta)$ in the Hilbert space $L^2(\mathbb{R}^+ \times S^1)$ with inner product:

$$\langle f, g \rangle = \int_0^\infty \int_0^{2\pi} f(r', \theta)\overline{g(r', \theta)}\, r'\, d\theta\, dr'.$$

18.2 The Logarithmic Laplacian Operator

We define the log-causal Laplacian $\Delta_{\log}$ as the scale-invariant Laplace–Beltrami operator in these coordinates:

$$\Delta_{\log} = \frac{\partial^2}{\partial x'^2} + \frac{\partial^2}{\partial t'^2} = \frac{\partial^2}{\partial r'^2} + \frac{1}{r'}\frac{\partial}{\partial r'} + \frac{1}{r'^2}\frac{\partial^2}{\partial \theta^2}.$$

Let $\mathcal{H} = -\Delta_{\log}$ act on a suitable dense domain $\mathcal{D} \subset L^2$. Then $\mathcal{H}$ is essentially self-adjoint and has purely real spectrum.

18.3 Radial Reduction and Spectral Problem

Assuming rotational symmetry, we consider radial eigenfunctions $\psi_n(r')$ satisfying:

$$\left(-\frac{d^2}{dr'^2} - \frac{1}{r'}\frac{d}{dr'}\right)\psi_n(r') = \lambda_n \psi_n(r').$$

We set:

$$\psi_n(r') = \frac{1}{\sqrt{r'}} u_n(\log r'),$$

and apply the change of variables $\rho = \log r'$. Then the equation becomes:

$$\left(-\frac{d^2}{d\rho^2} + V(\rho)\right) u_n(\rho) = \lambda_n u_n(\rho),$$

where $V(\rho)$ includes an effective centrifugal term. The operator is now of Sturm–Liouville form on a log-compactified domain.

18.4 Connection to the Riemann Zeros

We conjecture that a modified operator of the form:

$$\mathcal{H}_\zeta = -\Delta_{\log} + \Phi(r'),$$

with a potential Φ encoding arithmetic symmetry, could have a spectrum whose imaginary parts correspond to nontrivial zeros of $\zeta(s)$:

$$\mathrm{Spec}(\mathcal{H}_\zeta) = \{\gamma_n\} \quad \text{where} \quad \zeta\left(\frac{1}{2} + i\gamma_n\right) = 0.$$

Such a $\Phi(r')$ might be constructed using the explicit formula of Riemann or trace formula analogs, linking spectral density to prime distributions.

18.5 Trace Formula and Prime Counting

Let $K(r', r')$ denote the heat kernel of $\mathcal{H}_\zeta$. A spectral trace over causal depth gives:

$$\mathrm{Tr}(e^{-t\mathcal{H}_\zeta}) = \sum_n e^{-t\gamma_n},$$

which may be compared to the explicit formula for the prime counting function $\pi(x)$ via inverse Laplace or Mellin transforms.

18.6 Conclusion and Open Path

The logarithmic spacetime framework provides a geometric Hilbert space, a self-adjoint operator, and a scale-covariant structure for encoding spectral properties of arithmetic zeta functions. Further

work is needed to explicitly construct the potential $\Phi(r')$ that generates the Riemann spectrum, possibly by leveraging modular or automorphic functions.

19 Summary and Outlook

19.1 Unified Geometric Framework

This work presents a theory in which spacetime is not linear but logarithmic in its fundamental causal coordinates:

$$x = e^{x'}, \quad t = e^{t'}, \quad c = e^{r'}$$

From this, observable phenomena such as redshift, time dilation, quantum uncertainty, and gravitational horizons are seen as projections from a deeper invariant structure. The model unifies quantum mechanics, general relativity, and cosmology within a single geometric architecture.

19.2 Experimental Roadmap

The following observations can critically test the theory:

- Luminosity distances vs. redshift: $(1+z)^2$ scaling
- Logarithmic corrections to quantum uncertainty at high energies
- Horizon-scale signatures in CMB and black hole ringdowns
- Running of the fine-structure constant with causal depth

These predictions are within reach of current or near-future experiments such as JWST, LISA, and the HL-LHC.

19.3 Paradigm Shift Potential

Log-spacetime offers:

- Natural regularization of infinities
- Geometric interpretation of constants and couplings
- A new synthesis between perception, measurement, and causal structure

It challenges foundational assumptions and reframes observed anomalies as natural consequences of projection from log-scale depth.

19.4 Conclusion

What appears as a vast, dynamic cosmos may instead be a narrow exponential window onto an infinitely deep causal geometry. This perspective may unify known physics and resolve open problems—not through new forces or particles, but by understanding that the world we observe is a projection on a logarithmic screen.

Conflict of Interest

The authors declare that there is no conflict of interest regarding the publication of this paper.

Data Availability

The data that support the findings of this study are available from the corresponding author upon reasonable request.

References

[1] B. P. Abbott et al., "Tests of General Relativity with Binary Black Holes from the LIGO–Virgo Catalog GWTC-2," *Phys. Rev. D*, vol. 103, no. 12, 2021.

[2] M. Alcubierre, "The warp drive: hyper-fast travel within general relativity," *Classical and Quantum Gravity*, vol. 11, no. 5, pp. L73–L77, 1994.

[3] G. Amelino-Camelia, "Doubly special relativity," Nature **418**, 34–35 (2002).

[4] A. Ashtekar, "Information is Not Lost in the Evaporation of Black Holes," *Phys. Rev. Lett.*, vol. 96, 2006.

[5] J. Benford, G. Benford, and D. Benford, "Messaging with Cost-Optimized Interstellar Beacons," *Astrobiology*, vol. 10, no. 5, pp. 491–498, 2010.

[6] W. Bialek, I. Nemenman, and N. Tishby, *Predictability, Complexity, and Learning*, Neural Computation 13, 2409–2463 (2001), arXiv:physics/0007070.

[7] P. Bosso, "Generalized Uncertainty Principle and Quantum Gravity Phenomenology," *Annalen der Physik*, vol. 530, no. 1, 2018.

[8] R. Brout et al., "Pantheon+ Analysis: The Complete Cosmological Constraints from Type Ia Supernovae," *ApJ*, vol. 938, no. 2, 2022.

[9] C. P. Burgess, "The Cosmological Constant Problem: Why it's hard to get Dark Energy from Micro-physics," in *100 Years of General Relativity*, World Scientific, 2013.

[10] R. R. Caldwell and M. Kamionkowski, *The Physics of Cosmic Acceleration*, Ann. Rev. Nucl. Part. Sci. **59**, 397–429 (2009).

[11] S. Carroll, "The Cosmological Constant," *Living Reviews in Relativity*, vol. 4, 2001.

[12] P. Delva et al., "Test of Special Relativity Using a Fiber Network of Optical Clocks," *Phys. Rev. Lett.*, vol. 118, no. 22, 2017.

[13] R. Descartes, *La Géométrie*, 1637.

[14] S. Doplicher, K. Fredenhagen, J. E. Roberts, *The Quantum Structure of Spacetime at the Planck Scale and Quantum Fields*, Commun. Math. Phys. 172, 187 (1995), arXiv:hep-th/0303037.

[15] G. T. Fechner, *Elemente der Psychophysik*, Breitkopf & Härtel, 1860.

[16] E. Fischbach and C. Talmadge, "Ten Years of the Fifth Force," *Nature*, vol. 356, 1992, pp. 207–215.

[17] L. J. Garay, "Quantum gravity and minimum length," *Int. J. Mod. Phys. A*, vol. 10, no. 2, pp. 145–165, 1995.

[18] A. Guth, "Inflationary universe: A possible solution to the horizon and flatness problems," *Phys. Rev. D*, vol. 23, no. 2, pp. 347–356, 1981.

[19] D. Harlow, "Jerusalem Lectures on Black Holes and Quantum Information," *Rev. Mod. Phys.*, vol. 88, 2016.

[20] S. W. Hawking, "Breakdown of predictability in gravitational collapse," Phys. Rev. D **14**, 2460 (1976).

[21] S. Hossenfelder, "Minimal length scale scenarios for quantum gravity," *Living Rev. Relativ.*, vol. 16, no. 2, 2013.

[22] S. Hossenfelder, *Lost in Math: How Beauty Leads Physics Astray*, Basic Books, 2018.

[23] A. Jaffe and E. Witten, "*Quantum Yang–Mills Theory*," The Millennium Prize Problems, Clay Mathematics Institute, 2000.

[24] A. Kempf, G. Mangano, and R. B. Mann, "Hilbert space representation of the minimal length uncertainty relation," *Phys. Rev. D*, vol. 52, 1108–1118, 1995.

[25] J. Kogut and L. Susskind, "*Hamiltonian formulation of Wilson's lattice gauge theories*," Phys. Rev. D **11**, 395 (1975).

[26] S. McGaugh et al., "Radial Acceleration Relation in Rotationally Supported Galaxies," *Phys. Rev. Lett.*, vol. 117, 2016.

[27] P. Minkowski, "$\mu \to e\gamma$ at a Rate of One Out of 1-Billion Muon Decays?," *Phys. Lett. B*, vol. 67, pp. 421–428, 1977.

[28] C. W. Misner, K. S. Thorne, and J. A. Wheeler, *Gravitation*. W. H. Freeman, 1973.

[29] J. Napier, *Mirifici Logarithmorum Canonis Descriptio*, 1614.

[30] T. Padmanabhan, "*Duality and zero-point length of spacetime*," Phys. Rev. Lett. **78**, 1854 (1997).

[31] T. Padmanabhan, "Understanding our Universe: Current status and open issues," *Current Science*, vol. 88, no. 7, pp. 1057–1066, 2005.

[32] S. Perlmutter et al., "Measurements of Ω and Λ from 42 High-Redshift Supernovae," *Astrophys. J.*, vol. 517, 565, 1999.

[33] M. E. Peskin and D. V. Schroeder, *An Introduction to Quantum Field Theory*, Westview Press (1995).

[34] H. E. Puthoff, "Zero-point energy as an energy source," *Phys. Rev. A*, vol. 40, no. 9, pp. 4857–4862, 1989.

[35] A. G. Riess *et al.*, *Large Magellanic Cloud Cepheid Standards Provide a 1% Foundation for the Determination of the Hubble Constant*, Astrophys. J. **876**, 85 (2019).

[36] A. G. Riess et al., "A Comprehensive Measurement of the Local Value of the Hubble Constant," *ApJ*, vol. 908, no. 1, 2021.

[37] W. Rindler, *Relativity: Special, General, and Cosmological*, 2nd ed. Oxford University Press, 2006.

[38] C. Rovelli, *Quantum Gravity*, Cambridge University Press, 2004.

[39] A. D. Sakharov, "Vacuum quantum fluctuations in curved space and the theory of gravitation," *Sov. Phys. Dokl.*, vol. 12, pp. 1040–1041, 1967.

[40] D. Scolnic et al., "The Pantheon+ Analysis: The Complete Supernova Dataset and Cosmological Constraints," *Astrophys. J.*, vol. 938, no. 2, 2022.

[41] C. L. Smith, *Logarithmic Spacetime and Causal Geometry: A New Framework for Scale-Invariant Physics*, 2025.

[42] S. S. Stevens, "On the psychophysical law," *Psychological Review*, vol. 64, no. 3, pp. 153–181, 1957.

[43] M. Takamoto et al., "Test of general relativity by a pair of transportable optical lattice clocks," *Nature Photonics*, vol. 14, pp. 411–415, 2020.

[44] J.-P. Uzan, "Varying Constants, Gravitation and Cosmology," *Living Rev. Relativity*, vol. 14, 2011.

[45] L. Verde, T. Treu, and A.G. Riess, *Tensions between the Early and the Late Universe*, Nature Astronomy **3**, 891–895 (2019).

[46] E. Verlinde, *On the Origin of Gravity and the Laws of Newton*, JHEP 2011, 029 (2011), arXiv:1001.0785.

[47] J. K. Webb et al., "Evidence for spatial variation of the fine structure constant," *Phys. Rev. Lett.*, vol. 107, 191101, 2011.

[48] S. Weinberg, "The Cosmological Constant Problem," *Rev. Mod. Phys.*, vol. 61, no. 1, 1989.

[49] S. Weinberg, *The Quantum Theory of Fields*, Vol. I, Cambridge University Press, 1995.

[50] M. Wittmann and M. Lehnhoff, "Age effects in perception of time," *Psychology and Aging*, vol. 24, no. 3, pp. 925–929, 2009.